Langmuir

Article

pubs.acs.org/Langmuir

Spectrum of Membrane Morphological Responses to Antibacterial Fatty Acids and Related Surfactants

Bo Kyeong Yoon,[†,‡] Joshua A. Jackman,[†,‡] Min Chul Kim,[†,‡] and Nam-Joon Cho*[,†,‡,§]

[†]School of Materials Science and Engineering and [‡]Centre for Biomimetic Sensor Science, Nanyang Technological University, 50 Nanyang Avenue 639798, Singapore

[§]School of Chemical and Biomedical Engineering, Nanyang Technological University, 62 Nanyang Drive 637459, Singapore

Supporting Information

ABSTRACT: Medium-chain saturated fatty acids and related compounds (e.g., monoglycerides) represent one class of membrane-active surfactants with antimicrobial properties. Most related studies have been in vitro evaluations of bacterial growth inhibition, and there is limited knowledge about how the compounds in this class destabilize lipid bilayers, which are the purported target within the bacterial cell membrane. Herein, the interaction between three representative compounds in this class and a supported lipid bilayer platform was investigated using quartz crystal microbalance-dissipation and fluorescence microscopy in order to examine membrane destabilization. The three tested compounds were lauric acid, sodium dodecyl sulfate, and glycerol monolaurate. For each compound, we discovered striking differences in the resulting morphological changes of supported lipid bilayers. The experimental trends indicate that the compounds have membrane-disruptive behavior against supported lipid bilayers principally above the respective critical micelle concentration values. The growth inhibition properties of the compounds against standard and methicillin-resistant *Staphylococcus aureus* bacterial strains were also tested. Taken together, the findings in this work improve our knowledge about how saturated fatty acids and related compounds destabilize lipid bilayers, offering insight into the corresponding molecular mechanisms that lead to membrane morphological responses.

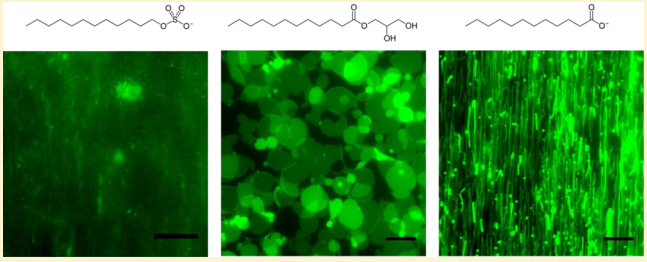

INTRODUCTION

Antibiotic resistance is one of the most serious public health issues in the world, sparked in part by the overuse of antibiotics in medicine and agriculture.[1] In the face of multi-drug-resistant bacteria, many antibiotics are losing effectiveness, and there is growing recognition that a postantibiotic era is approaching.[2] To address this issue, there has been renewed attention on antimicrobial lipids which act as mild surfactants that damage bacterial cell membranes.[3] While antibiotics interfere with specific processes in the bacterial life cycle (e.g., inhibit enzymes involved in cell wall synthesis) that leave them prone to the evolution of antibiotic-resistant bacterial strains,[4] certain lipids, and more broadly surfactants in general, act promiscuously in order to target the bacterial cell membrane and can exhibit bacteriostatic or bactericidal effects.[5] Partial solubilization of the cell membrane interferes with metabolic regulation, leading to the inhibition of bacterial growth. On the other hand, membrane lysis irreversibly damages a bacterium and causes cell death, often quickly on the time scale of minutes. Owing to the multiple ways by which antimicrobial lipids target bacterial cell membranes, there is a high barrier to the emergence of drug-resistant bacterial strains.[6]

At the same time, the promiscuity of antimicrobial lipids can have deleterious effects on host cell membranes, and surfactants either in free form[7] or emulsions[8] have been primarily used as topical microbicides or in industrial applications (e.g., food preservatives). Liposomal formulations have also been developed[9−14] in order to encapsulate fatty acids, offering a delivery vehicle that minimizes host cell toxicity and other deleterious side effects while showing therapeutic promise to reduce bacterial loads in in vitro and in vivo studies, including for both topical and systemic administration routes. Small liposomes loaded with fatty acids in the bilayer can fuse with the bacterial cell membrane, leading to the release of high local concentrations of fatty acids into the bacterial cell membrane which results in gross morphological changes and enhanced membrane permeability that cause bacterial cell death.[13] In all embodiments—free form, emulsion, or liposome—the key contributing factor to antibacterial activity is the antimicrobial lipid itself, and there is great interest in understanding how lipids and surfactants interfere with bacterial cell membranes.

To date, numerous antimicrobial lipids and structurally related surfactants have been discovered or synthesized with variable efficacies and spectra. In order to understand how the chemical structure of a lipid influences its antimicrobial properties, extensive in vitro studies have been conducted

Received: June 8, 2015
Revised: August 3, 2015
Published: September 1, 2015

DOI: 10.1021/acs.langmuir.5b02088
Langmuir 2015, 31, 10223−10232

and open the door to mechanistic investigations. Kabara and colleagues led pioneering studies on the antibacterial properties of medium-chain saturated fatty acids.[15−17] Through systematic investigation of saturated fatty acids with chain lengths of between 6 and 18 carbons, it was determined that lauric acid has the most potent inhibitory activity against Gram-positive bacteria.[18] The 1-monoglyceride derivative of lauric acid is called glycerol monolaurate and was discovered to have a lower minimum inhibitory concentration than lauric acid, albeit against a narrower range of bacteria.[19] Both lauric acid and glycerol monolaurate (GML) are generally recognized as safe by the United States Food and Drug Administration and are used as food preservatives and cosmetic emulsifiers.[20] Another related compound is sodium dodecyl sulfate (SDS), which is widely used as a detergent with known antimicrobial properties.[21] As presented in Figure 1, all three compounds share a 12-carbon-long primary alkyl chain and have different headgroups that influence the corresponding physicochemical properties.

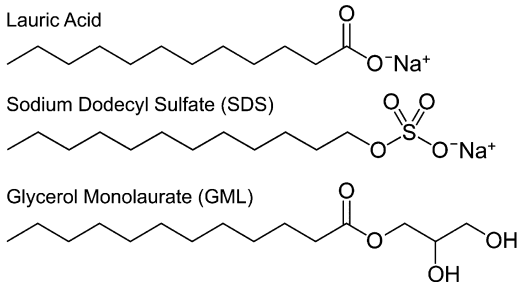

Figure 1. Chemical structure of tested antimicrobial lipids. Lauric acid, glycerol monolaurate, and SDS each have a 12-carbon-long primary alkyl chain. The critical micelle concentrations of the surfactants in aqueous solution are lauric acid (1.5 mM, ref 25), glycerol monolaurate (42 μM, ref 26), and SDS (260 μM, ref 26). The quoted CMC values were obtained from literature reports which investigated the surfactants under high-ionic-strength aqueous conditions comparable to the conditions used in this study.

While the structure−activity relationships of fatty acids and related compounds have been investigated in terms of bacterial growth inhibition, it remains to be understood how treatment with these compounds affects the properties of lipid membranes. Indeed, surfactants in general encompass a spectrum of mechanistic behaviors (e.g., permeabilization, lysis, etc.), with the molecular-level details depending on the physicochemical properties and concentration of the surfactant.[22] Thus far, there have been extensive mechanistic studies of cationic amphiphiles, especially membrane-active peptides, but specific modes of action remain to be defined, in part reflecting the complexity of studying biological systems.[23] Scanning electron microscopy has been employed to visualize fixed specimens of bacteria after treatment with high concentrations of certain fatty acids and derivatives.[24] However, to our knowledge, there has been no direct investigation of the membrane destabilization process for saturated fatty acids and related compounds.

As a representative model of cell membranes, the supported lipid bilayer platform has proven useful in order to evaluate the interfacial activity of other classes of membrane-active compounds, including phospholipase enzymes[27] and the aforementioned cationic antimicrobial peptides.[28] Importantly, the platform is compatible with a wide range of surface-sensitive measurement techniques such as label-free acoustic and optical sensors as well as fluorescence microscopy and atomic force microscopy techniques which enable a detailed examination of lipid bilayer properties during treatment with membrane-active compounds.[29] Such capabilities are well-suited to investigate the dynamic processes by which medium-chain saturated fatty acids and related compounds destabilize lipid bilayers.

The goal of the present study was to compare how lauric acid, GML, and SDS affect the physical properties of supported lipid bilayers. Quartz crystal microbalance-dissipation (QCM-D) and fluorescence microscopy experiments were employed in order to monitor changes in the mass, viscoelastic, and morphological properties of the supported lipid bilayer upon treatment with compounds at various concentrations. This approach provided a quantitative measurement framework in order to compare the interfacial activity of the different compounds. The bacterial growth inhibition properties of each compound were also tested against standard and methicillin-resistant *Staphylococcus aureus*, a Gram-positive bacterium which is a leading cause of antibiotic-resistant infections in humans,[30] by determining minimum inhibitory concentration (MIC) values. Collectively, the findings present evidence that the tested compounds differentially act against supported lipid bilayers, offering insight into how these compounds interfere with lipid membranes and induce membrane morphological changes.

EXPERIMENTAL SECTION

Materials. 1,2-Dioleoyl-*sn*-glycero-3-phosphocholine (DOPC) was purchased from Avanti Polar Lipids, Inc. (Alabaster, AL). Lauric acid, sodium dodecyl sulfate, Mueller-Hinton (MH) agar, and Mueller-Hinton broth were obtained from Sigma-Aldrich (St Louis, MO). Glycerol monolaurate was purchased from Abcam (Cambridge, U.K.). Luria-Bertani (LB) broth was purchased from BD (Sparks, MD). Phosphate-buffered saline (PBS) was purchased from Gibco (Carlsbad, CA). All solutions were prepared with Milli-Q-treated water (>18 MΩ·cm) (Millipore, Billerica, MA).

Preparation of Antimicrobial Lipid Solutions. The desired mass of antimicrobial lipid powder was weighed using an analytical balance. Stock solutions of lauric acid and GML were prepared by first dissolving the weighed compounds in ethanol to a final concentration of 200 mM. In order to prepare lauric acid and GML test samples, an aliquot from the stock solution was diluted 1:100 with phosphate buffer (PB), phosphate-buffered saline (PBS), or Mueller-Hinton (MH) broth. The concentration of the diluted compound was 2 mM. SDS test samples were prepared by dissolving the weighed compound in the appropriate media (without the ethanol step) to a concentration of 2 mM. To increase the solubility of all test samples, the solutions were heated in a 70 °C water bath for 30 min. Subsequent dilutions were made in accordance with the experimental protocols. The maximum concentration of ethanol at the highest test concentration was 1% in aqueous solution, and lauric acid (pK_a ∼5) and SDS (pK_a ∼2) are assumed to be deprotonated under all test conditions. All solutions were prepared on the same day as the experiments. The dry compounds were stored in a dark cabinet.

Quartz Crystal Microbalance-Dissipation (QCM-D) Experiments. QCM-D experiments with a Q-Sense E4 instrument (Q-Sense AB, Gothenburg, Sweden) were conducted in order to characterize the interaction between the test compounds and a supported lipid bilayer. The QCM-D technique monitors changes in the resonance frequency (Δf) and energy dissipation (ΔD) of an oscillating, piezoelectric quartz crystal sensor chip as functions of time, which reflect the acoustic mass and viscoelastic properties, respectively, of an adsorbate on the surface.[31] The sensor chip had a fundamental frequency of 5 MHz and a sputter-coated, 50-nm-thick layer of silicon dioxide (model no. QSX 303, Q-Sense AB). Before the experiment, the sensor chips were sequentially rinsed with water and ethanol, dried with nitrogen gas, and subjected to oxygen plasma treatment for 1 min with an Expanded

DOI: 10.1021/acs.langmuir.5b02088
Langmuir 2015, 31, 10223−10232

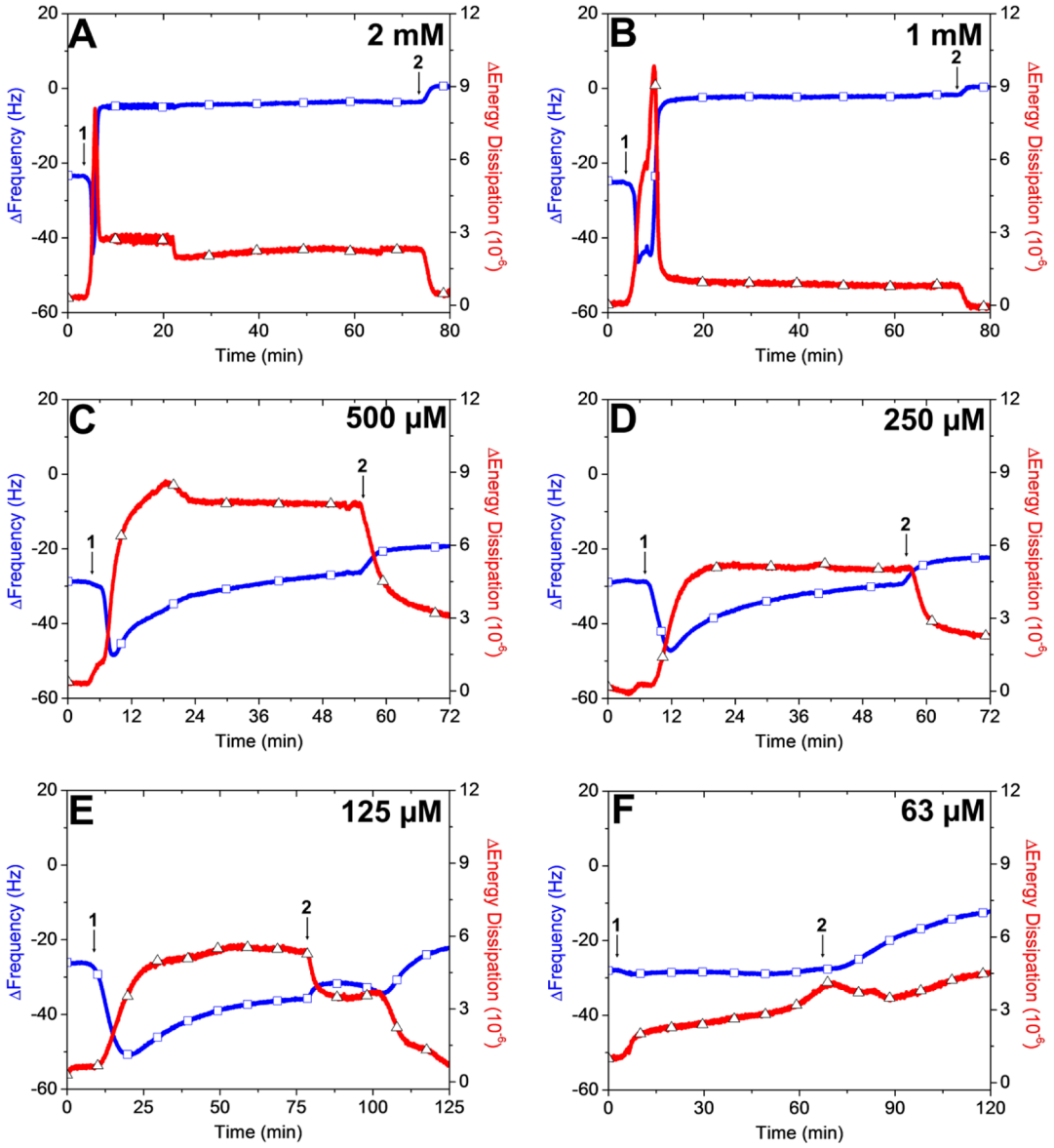

Figure 2. QCM-D investigation of SDS treatment on supported lipid bilayers. Δf (blue line with squares) and ΔD (red line with triangles) shifts as functions of time are presented for (A) 2 mM, (B) 1 mM, (C) 500 μM, (D) 250 μM, (E) 125 μM, and (F) 63 μM SDS. The initial measurement values correspond to a supported lipid bilayer on the silicon dioxide surface. SDS was added at t = 5 min (arrow 1), and a washing step was performed (arrow 2) after the measurement signals stabilized.

Plasma Cleaner (model no. PDC-002, Harrick Plasma, Ithaca, NY). In the experiments, a supported lipid bilayer composed of a 1,2-dioleoyl-*sn*-glycero-3-phosphocholine (DOPC) lipid was initially formed using the solvent-assisted lipid bilayer (SALB) technique.[32] Briefly, a baseline signal was recorded in aqueous buffer solution (10 mM Tris, 150 mM NaCl, pH 7.5) and then substituted with isopropanol solution. Next, a 0.5 mg/mL DOPC lipid in isopropanol solution was added and allowed to equilibrate for 10 min followed by exchange with aqueous buffer solution in order to form the supported lipid bilayer. Finally, 50 μM bovine serum albumin (BSA) was added as a blocking agent in order to prevent the nonspecific adsorption of antibacterial agents in subsequent steps. After the bilayer formation process was completed, the solution was exchanged with PBS solution, and then the test compound in an identical PBS solution was added under continuous flow conditions for a minimum of 30 min. A washing step with PBS solution completed the procedure. In all steps, a peristaltic pump (Reglo Digital, Ismatec, Glattbrugg, Switzerland) was used to inject liquid samples into the measurement chamber at a flow rate of 50 μL/min. During the experiments, the temperature in the measurement cell was maintained at 25.0 ± 0.5 °C. The experimental data was collected at the third (n = 3), fifth (n = 5), and seventh (n = 7) odd overtones using the QSoft (Q-Sense AB) software package, and the data was normalized according to the overtone number. Data processing was performed in the QTools (Q-Sense AB) and OriginPro 8.5 (OriginLab, Northampton, MA) software packages. All presented data was collected at the fifth overtone.

Fluorescence Microscopy Experiments. Epifluorescence microscopy was performed in order to directly observe morphological changes in supported lipid bilayers due to treatment with the test compounds. An Eclipse TI-U inverted optical microscope (Nikon, Japan) with a 60× magnification (NA = 1.49) oil-immersion objective lens (Nikon) was used, and images were recorded with an iXon 512 pixel × 512 pixel EMCCD camera (Andor Technology, Northern Ireland). The pixel size was 0.267 × 0.267 μm^2. A fiber-coupled mercury lamp (Intensilight C-HGFIE, Nikon) was used to illuminate the fluorophores with a TRITC filter. Initially, supported lipid bilayers were formed by the vesicle fusion method (0.2 mg/mL extruded DOPC lipid vesicles with 68 nm diameter; see ref 33) inside a

DOI: 10.1021/acs.langmuir.5b02088
Langmuir 2015, 31, 10223−10232

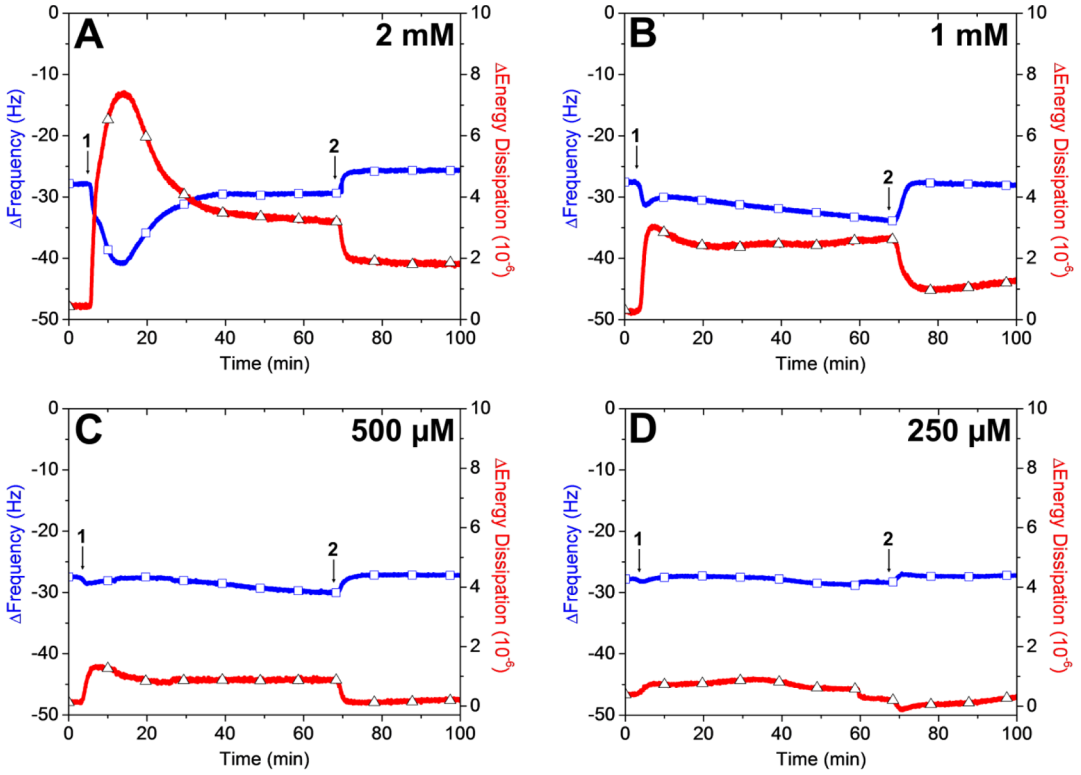

Figure 3. QCM-D investigation of lauric acid treatment on supported lipid bilayers. Δf (blue line with squares) and ΔD (red line with triangles) shifts as functions of time are presented for (A) 2 mM, (B) 1 mM, (C) 500 μM, and (D) 250 μM lauric acid. The initial measurement values correspond to a supported lipid bilayer on the silicon dioxide surface. Lauric acid was added at t = 5 min (arrow 1), and a washing step was performed (arrow 2) after the measurement signals stabilized.

microfluidic flow-through chamber (sticky slide VI 0.4, Ibidi, Germany). After formation, the lipid bilayer was rinsed with buffer solution, and then the test compound was introduced into the measurement chamber at a flow rate of 40 μL/min. During this stage, time-lapse images were recorded every 5 s for a total duration of 30 min. The initial time, t = 0 s, was defined by when the test compound solution reached the channel inlets. For each measurement recorded, the fluorescence intensity of each image was normalized using a custom-written script for the Python(x,y) 2.7.5 software program.

Bacterial Cell Culture. *S. aureus* (ATCC 25923) and methicillin-resistant *S. aureus* (ATCC 33591) (American Type Culture Collection, Manassas, VA) were cultured in LB broth overnight at 37 °C. The suspension of the overnight culture was inoculated in fresh LB broth and cultured under aerobic conditions until reaching an OD_{600} value of approximately 0.5 (exponential growth phase). The bacterial cells were harvested by centrifugation at 1500*g* for 10 min, washed three times with PB or PBS, and resuspended in the appropriate solution for the experiment. The bacterial cell suspensions were diluted to an OD_{600} value of 0.1, which corresponds to 1×10^7 CFU/mL for *S. aureus*.[34] Before the experiment, the bacterial cells were then diluted 1:10 with PB, PBS, or MHB.

Minimum Inhibitory Concentration (MIC) Testing. The MIC values of the test compounds were determined in PB, PBS, and MH broth solutions.[35] For the PB and PBS cases, the MIC determination was made by a MH agar plate method. Twofold serial dilutions of test compound solutions in PB or PBS were first made in a 96-well microtiter plate. The test compound concentration ranged from 8 μM to 1 mM with a 50 μL volume. Then, 50 μL of *S. aureus* (1×10^6 CFU/mL) suspended in PB or PBS was added to each well for a final cell density of 5×10^5 CFU/mL. The samples were incubated for 3 h at 37 °C and then streaked onto MH agar plates. The plates were incubated overnight at 37 °C, and the MIC value was recorded on the basis of the lowest test compound concentration that inhibited colony growth. For the MH broth case, the MIC determination was made by the broth microdilution method. Twofold serial dilutions of test compound solutions in MH broth were first made in a 96-well microtiter plate. The test compound concentration ranged from 4 μM to 2 mM with a 75 μL volume. Then, 75 μL of *S. aureus* (1×10^6 CFU/mL) suspended in MH broth was added to each well for a final cell density of 5×10^5 CFU/mL. The samples were incubated with shaking for 24 h at 37 °C. After incubation, the MIC value was recorded by OD_{600} measurement using a microplate reader.

RESULTS

Effect on Mass and Viscoelastic Properties of Supported Lipid Bilayers. To investigate the effect of the test compounds on lipid bilayers, supported lipid bilayers on silicon dioxide surfaces were initially formed using the solvent-assisted lipid bilayer (SALB) formation method.[32] The single-component lipid bilayers were made of zwitterionic DOPC lipid. The QCM-D technique was employed in order to monitor the bilayer fabrication process, and the experimental protocol consistently yielded supported lipid bilayers with final Δf and ΔD shifts of -26 ± 2 Hz and $0.3 \pm 0.2 \times 10^{-6}$, respectively. These values are in good agreement with expected values for a supported lipid bilayer,[36] as further confirmed by a bovine serum albumin (BSA) blocking step. BSA protein exhibits significant adsorption on hydrophilic silicon dioxide but not on zwitterionic lipid bilayers.[37] A large reduction in BSA adsorption to the bilayer-coated substrates was observed in comparison to bare substrates, supporting that the lipid bilayers form homogeneous and complete (>95%) thin films. After fabrication, the supported lipid bilayers were exposed to a flow-through sample of test compound with a fixed bulk concentration, as monitored by the QCM-D technique. The measurement results obtained for each compound are described below. In Figures 2–4, note that the initial baseline

DOI: 10.1021/acs.langmuir.5b02088
Langmuir 2015, 31, 10223–10232

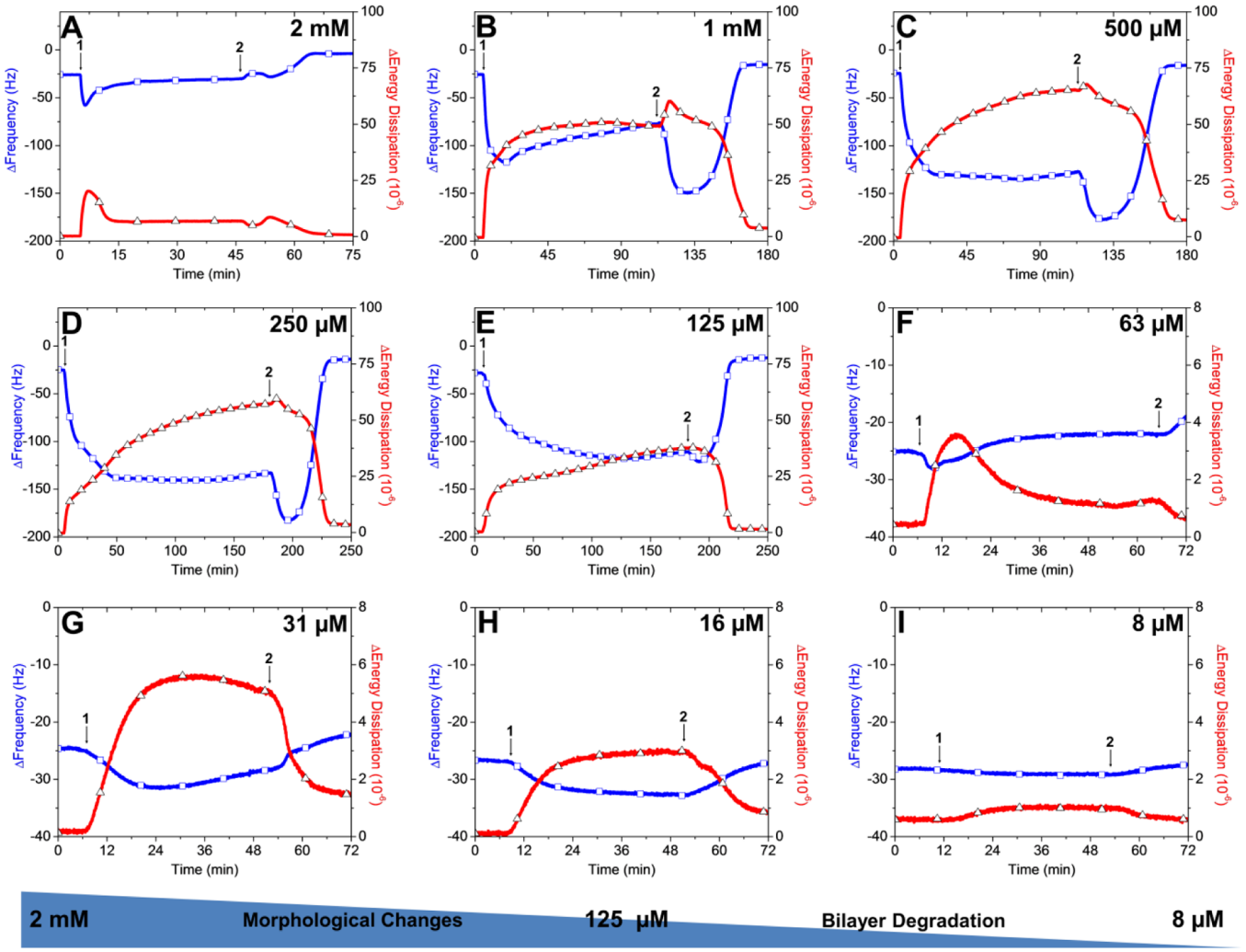

Figure 4. QCM-D investigation of GML treatment on supported lipid bilayers. Δf (blue line with squares) and ΔD (red line with triangles) shifts as functions of time are presented for (A) 2 mM, (B) 1 mM, (C) 500 μM, (D) 250 μM, (E) 125 μM, (F) 63 μM, (G) 31 μM, (H) 16 μM, and (I) 8 μM GML. The initial measurement values correspond to a supported lipid bilayer on the silicon dioxide surface. GML was added at t = 5 min (arrow 1), and a washing step was performed (arrow 2) after the measurement signals stabilized.

values for the Δf and ΔD shifts correspond to supported lipid bilayer formation.

Sodium Dodecyl Sulfate. Figure 2 presents the effects of SDS on the Δf and ΔD shifts as functions of SDS concentration. At 1 mM and higher SDS concentrations, there was a rapid decrease in Δf to around −45 Hz that was mirrored by an increase in ΔD to around 9×10^{-6} (Figure 2A,B). The transient spikes were quickly diminished, leading to final Δf and ΔD values of around −4 Hz and 1.5×10^{-6}, respectively. A washing step entirely removed lipid and SDS from the substrate, as indicated by final Δf and ΔD values of around 0 Hz and 0×10^{-6}, respectively.

At lower SDS concentrations between 125 and 500 μM, similar initial decreases in Δf to around −47 Hz were observed, and the time required to reach the inflection point was inversely proportional to the bulk SDS concentration (Figure 2C−E). The Δf values nearly stabilized at around −30 to −39 Hz over a longer time. On the other hand, in this concentration range, the ΔD shift did not correlate with the Δf shift. Rather, there was a monotonic increase in ΔD that weakly increased with SDS concentration, from 5×10^{-6} at 125 μM to 8×10^{-6} at 500 μM. Upon washing, the Δf values increased to around −22 to −25 Hz, and the ΔD values decreased to between 1×10^{-6} and 4×10^{-6}.

At 63 μM SDS, there was a negligible change in Δf and a minor increase in ΔD to around 3×10^{-6} (Figure 2F). A washing step led to a moderate increase in Δf to approximately −14 Hz and a negligible change in the ΔD value. Taken together, 1 mM and higher SDS concentrations induced complete solubilization of the lipid bilayer through a transient stage of membrane perturbation, while lower SDS concentrations induced changes in the lipid bilayer without complete solubilization.

Lauric Acid. Figure 3 presents the effects of lauric acid on the Δf and ΔD shifts as functions of lauric acid concentration. At 2 mM lauric acid concentration, there was a simultaneous decrease in Δf and an increase in ΔD to −42 and 7×10^{-6}, respectively (Figure 3A). The Δf shift returned upward to around −31 Hz while the ΔD shift decreased and stabilized at around 3×10^{-6}. A washing step led to the Δf and ΔD shifts reaching −27 Hz and 2×10^{-6}, respectively. At 1 mM lauric acid concentration, there was a minor decrease in Δf to −31 Hz and an increase in ΔD to 3×10^{-6} (Figure 3B). A washing step led to an increase in Δf to −27 Hz and a decrease in ΔD to 1.2

DOI: 10.1021/acs.langmuir.5b02088
Langmuir 2015, 31, 10223−10232

$\times 10^{-6}$. Similar, although markedly attenuated, results were observed at 500 μM lauric acid, and there were negligible changes for 250 μM lauric acid (Figure 3C,D). Hence, lauric acid affected the measured properties of the lipid bilayer only at high concentrations, and lower concentrations had minimal effects on the lipid bilayer.

Glycerol Monolaurate. Figure 4 presents the effects of GML on the Δf and ΔD shifts as functions of GML concentration. At 2 mM GML, there was a rapid drop in Δf to −59 Hz and a corresponding increase in ΔD to 21 $\times 10^{-6}$. The Δf and ΔD values stabilized at around −33 Hz and 8 $\times 10^{-6}$, respectively (Figure 4A). A washing step led to an increase in the Δf shift to −5 Hz and a decrease in the ΔD shift to around 0 $\times 10^{-6}$. By contrast, at 1 mM GML, a more gradual but appreciable decrease in Δf reached −118 Hz before incrementally rising to around −90 Hz (Figure 4B). The corresponding ΔD shift increased monotonically to approximately 48 $\times 10^{-6}$. A washing step led to a pronounced decrease in Δf to around −145 Hz before quickly increasing to −12 Hz. In this stage, the ΔD shift more closely paralleled the Δf shift with an increase to 56 $\times 10^{-6}$ followed by a decrease to 2 $\times 10^{-6}$. Similar trends were observed down to 250 μM GML with even larger Δf and ΔD shifts reaching up to −180 Hz and 64 $\times 10^{-6}$, respectively (Figure 4C,D).

At lower concentrations, the effect of GML on lipid bilayers was less pronounced but still significant. At 125 μM GML, there were simultaneous Δf and ΔD shifts that stabilized at around −108 Hz and 34 $\times 10^{-6}$, respectively (Figure 4E). A washing step reduced the Δf and ΔD shifts to final values of −10 Hz and 1 $\times 10^{-6}$, respectively. Between 63 and 16 μM GML, appreciably smaller effects on the lipid bilayer were detected (Figure 4F−H). The Δf and ΔD shifts reached −32 Hz and 4 $\times 10^{-6}$, respectively, largely independent of GML concentration in this regime. Washing steps indicated that the final Δf and ΔD shifts were minor. At 8 μM GML, there was no discernible effect on the lipid bilayer (Figure 4I). Taken together, the results indicate that GML has pronounced activity at 125 μM and higher, moderate activity between 63 and 16 μM, and minimal activity at 8 μM and below.

Observation of Morphological Changes in Supported Lipid Bilayers. In order to visualize morphological changes in the supported lipid bilayer, fluorescence microscopy experiments were also performed. The lipid composition was 99.5 mol % DOPC lipid and 0.5 mol % 1,2-dipalmitoyl-*sn*-glycero-3-phosphoethanolamine-*N*-(lissamine rhodamine B sulfonyl) lipid. The experiments were conducted in a flow-through microfluidic chamber in order to facilitate the addition of test compounds, as followed by fluorescence microscopy with time-lapse recording. Note that t = 0 s corresponds to the time when the test compound reached the measurement chamber. On the basis of the QCM-D measurements, specific concentrations of each compound were selected for further investigation based on the conditions which yielded significant changes in the measured properties of the lipid bilayers. The selected concentrations were 2 mM for SDS and lauric acid, and 500 μM for GML. The experimental results obtained for each compound are described below.

Sodium Dodecyl Sulfate. As shown in Figure 5, tubule formation followed by bilayer solubilization was induced by SDS (Video S1 in Supporting Information). Bright spots became visible on the lipid bilayer within 15 s and depict nucleation sites for tubular protrusions. The time scale of protrusion growth varied significantly, with some fibrils quickly growing to over 20 μm length within 75 s while other fibrils did not grow appreciably. Due to the continuous flow conditions, the tubules were oriented in one direction and some continued to grow. In due course, there was a pronounced decrease in the fluorescence intensity on the substrate indicative of lipid removal, and complete solubilization of the lipid bilayer, indicated by the lack of fluorescence intensity on the substrate, was observed within 10 min.

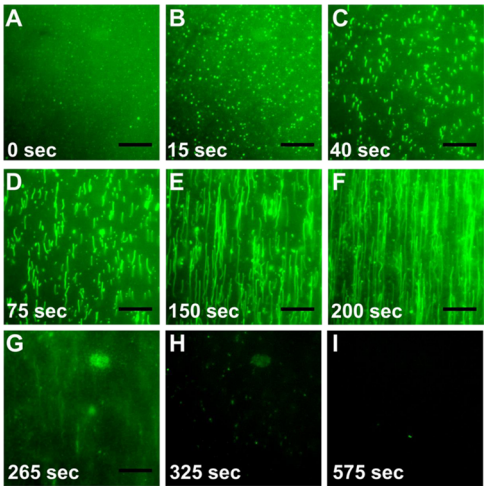

Figure 5. Microscopic observation of SDS-induced solubilization of supported lipid bilayers. (A−I) Image snapshots at various time points during SDS introduction depict nucleation sites that promote tubule formation followed by complete solubilization of the lipid bilayer. t = 0 s corresponds to the introduction of 2 mM SDS solution into the measurement chamber. The scale bars are 20 μm.

Lauric Acid. Figure 6 demonstrates that lauric acid also induces tubule formation on the lipid bilayer (Video S2 in Supporting Information). Bright spots were visible within 50 s and represented nucleation sites for the tubular protrusions, similar to the SDS case. Again, due to the flow conditions, the

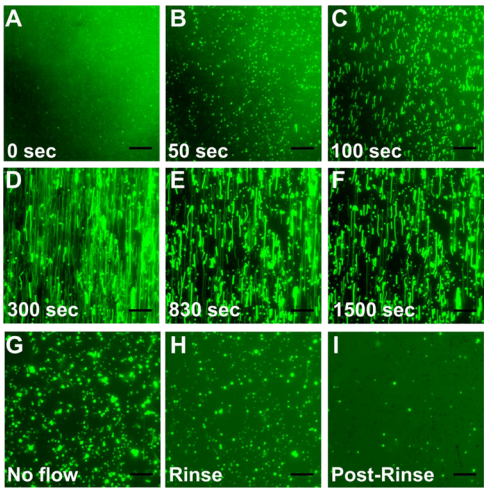

Figure 6. Microscopic observation of lauric acid-induced tubule formation on supported lipid bilayers. (A−F) Image snapshots at various time points depict nucleation sites from which stable tubules grow. t = 0 s corresponds to the introduction of 2 mM lauric acid solution into the measurement chamber. (G) Image snapshot after the flow was stopped. (H, I) Image snapshots show the effects of buffer rinsing, including tubule lysis and the appearance of fluorophore-poor domains. The scale bars are 20 μm.

DOI: 10.1021/acs.langmuir.5b02088
Langmuir 2015, 31, 10223−10232

tubules were oriented in one direction. A dense coverage of tubules was reached within 5 min. With increasing time, the number of tubules decreased, likely due to the detachment of some tubules from the lipid bilayer. However, complete solubilization of the lipid bilayer was not observed. Instead, most tubules remained stably attached for more than 30 min. After the flow was stopped, the parallel orientation of the tubules was lost and replaced by an out-of-plane orientation. Upon a buffer wash, nearly all tubular protrusions were removed from the lipid bilayer, and numerous defects (or phrase-separated domains) in the lipid bilayer were apparent, as denoted by fluorophore-poor regions which persisted over time (Video S3).

Glycerol Monolaurate. In contrast to the morphological changes induced by SDS and lauric acid, GML incorporation led to the formation of spherical protrusions in lipid bilayers, as presented in Figure 7 (Video S4 in Supporting Information).

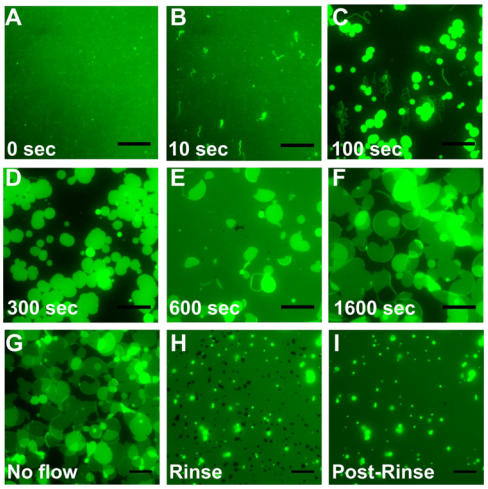

Figure 7. Microscopic observation of GML-induced spherical protrusions on supported lipid bilayers. (A–F) Image snapshots at various time points depict nucleation sites from which entangled tubules grow and form spherical caps. t = 0 s corresponds to the introduction of a 500 μM GML solution into the measurement chamber. (G) Image snapshot after the flow was stopped. (H, I) Image snapshots show the effects of buffer rinsing, including cap lysis as well as the appearance and disappearance of fluorophore-poor regions. The scale bars are 20 μm.

Within 10 s, the nucleation of tubular protrusions was initially observed. However, the tubules were not oriented in the flow direction. Rather, the individual tubules became self-entangled and, in some cases, entangled with adjacent tubules as well. Within 2 min, the entangled tubules disappeared and numerous expanding spherical protrusions were visible. More spherical protrusions formed and coalesced. After the flow was stopped, the spherical protrusions remained stable for at least 10 min. Upon a buffer wash, many of the spherical protrusions were removed from the lipid bilayer within 8 min, although some bright spots remained (Video S5). With continued washing, fluorophore-poor regions became visible in the lipid bilayer. After the buffer wash was stopped, the fluorophore-poor regions quickly disappeared within 2 min, resulting in uniform fluorescence intensity in the surrounding vicinity (Video S6). This observation lends credence to the possibility that, in this case, the fluorophore-poor regions correspond to GML-rich domains which mix with other components in the lipid bilayer, in effect demonstrating self-healing properties. It should be noted, however, that numerous bright spots remained stable and did not change over time.

Microbicidal Activity against *S. aureus* Bacteria. To further investigate how the surfactant concentration influences the microbicidal activity, MIC determinations were conducted under different solution conditions against one *S. aureus* bacterial strain (ATCC 25923) (Table 1). In low-salt PB solution, MIC values of 500 μM and 1 mM were recorded for SDS and lauric acid, respectively, while GML had a variable MIC value in the range of 15–63 μM depending on the individual experiment. In high-salt PBS solution, both SDS and lauric acid maintained similar MIC values. The MIC value of GML was 31 μM. Finally, MIC values were also recorded in Mueller-Hinton (MH) broth, which is a growth medium for microorganisms. In this case, the MIC value for GML was 125 μM while lauric acid and SDS had values of 500 μM and 1 mM, respectively. The MIC values obtained in MH broth solution agree well with reported literature values and trends (see, e.g., ref 18.). Similar results in MH broth were also obtained with a methicillin-resistant *S. aureus* strain (ATCC 33591). Consistent with the supported lipid bilayer experiments, the MIC values of GML were lower than those of lauric acid and SDS, supporting that GML is a more potent membrane-active compound.

Table 1. MIC Values for Antimicrobial Lipids against *S. aureus* Bacteria[a]

condition	lauric acid	SDS	GML
PB solution[b]	1 mM	500 μM	15–63 μM
PBS solution[b]	1 mM	500 μM	31 μM
MH broth[b]	500 μM	1 mM	125 μM
MH broth[c]	250 μM	1 mM	125 μM

[a]The MIC values are reported from a minimum of three independent experiments using a 2-fold-dilution protocol. [b]Standard *S. aureus* bacterial strain (ATCC 25923). [c]Methicillin-resistant *S. aureus* bacterial strain (ATCC 33591). Unless otherwise noted, identical results were obtained in all experiments. The only exception was GML experiments in PB solution for which there were variable results between 15 and 63 μM (36 ± 24 μM).

DISCUSSION

Supported Lipid Bilayer as an Experimental Platform. An experimental objective of this work was to utilize a model system in order to directly compare the effects of three antimicrobial lipids on membrane properties. Previous studies have investigated the antibacterial properties of all three test compounds by determining MIC values obtained in in vitro experiments, although there are outstanding questions about how factors such as the bacterial strain and solubilization conditions influence the measurement readout. For example, the recorded MIC value of lauric acid against *S. aureus* bacterial strains varies by 1 order of magnitude in the literature.[38] This variability in turn limits the quantitative comparison of literature MIC values for different antimicrobial lipids.

To address this issue, we have employed supported lipid bilayers as a standardized experimental platform that can be investigated with a wide range of surface-sensitive measurement techniques. QCM-D experiments were conducted in order to determine the effect of test compounds on the mass and viscoelastic properties of the supported lipid bilayer, while fluorescence microscopy experiments provided information

DOI: 10.1021/acs.langmuir.5b02088
Langmuir 2015, 31, 10223–10232

about morphological changes arising from treatment with the test compounds. For each compound, the two techniques showed excellent agreement in the measurement readouts and distinguished specific molecular-level behaviors, which varied considerably. SDS addition led to an initially large dissipation shift accompanied by a more moderate frequency shift that is consistent with the formation of out-of-plane tubules, as previously reported for another lipid bilayer system,[39] and both techniques also provided conclusive evidence for the eventual complete solubilization of the lipid bilayer. Similar trends in tubule formation were observed with lauric acid addition as well, albeit in different concentration ranges and without subsequent membrane solubilization. The behavior of lauric acid is similar to that observed with docosahexaenoic acid, a 22-carbon-long polyunsaturated fatty acid, when added to supported lipid bilayers.[40] On the other hand, GML addition led to striking differences in the measurement responses, with large frequency shifts and even larger dissipation shifts that are consistent with the formation of spherical caps protruding from the lipid bilayer. Taken together, the supported lipid bilayer investigations demonstrate that each of the three test compounds has a specific mechanism of action for membrane disruption.

Physicochemical Basis for Morphological Changes. In order to explain why the different fatty acids and derivatives have variable effects on the lipid bilayer morphology, one must take into account the physicochemical properties of the compounds. While all three compounds have a 12-carbon-long primary alkyl chain, lauric acid and SDS are anionic surfactants whereas GML is a nonionic surfactant. After amphiphilic compounds insert into the outer leaflet of the bilayer, the compounds can equilibrate by translocating into the inner leaflet.[3] For nonionic surfactants, the time scale is typically rapid (milliseconds to seconds), while the time scale is appreciably longer (hours to days) for charged surfactants.[41] Asymmetric insertion gives rise to a monolayer curvature strain,[3] leading to mechanical failure that can cause membrane morphological changes.

In another study, a general mechanical model was recently proposed by Staykova et al. in order to describe how confined lipid bilayers passively regulate stress by nucleating and evolving protrusions of varying geometries.[42] With increasing membrane strain, the protrusions that were formed shift from tubes to caps. The general trends predicted by this model are consistent with the present experimental observations that GML insertion induces less membrane strain than the tested anionic surfactants. Our observation of the coalescence of small buds into larger ones is also consistent with tension relief.[42] On the other hand, lauric acid and SDS insertion induce particularly high membrane strain due to slow translocation of the surfactant. SDS has greater positive spontaneous curvature than lauric acid due to a larger headgroup,[43] which is consistent with membrane solubilization only in the case of SDS treatment. Overall, the experimentally observed trends in membrane morphological changes are strongly correlated with the physicochemical properties of the surfactants and support that saturated fatty acids and related compounds can elicit a range of membrane perturbations depending on the molecular properties.

Role of Surfactant Concentration in Membrane Disruption. Another observation reported in this work is that all three tested compounds principally disturb supported lipid bilayers at or above the respective critical micelle concentration (CMC). This observation helps to explains why GML causes gross morphological changes in supported lipid bilayers at lower concentrations than for lauric acid and SDS. Importantly, the observation also leads to the key finding that the concentration of the test compound influenced the extent of membrane disruption in the supported lipid bilayer platform but did not affect the specific mechanism of action. While SDS induced complete membrane lysis resulting in structural disintegration, lauric acid and GML did not fully lyse the supported lipid bilayer. Hence, the range of membrane-lytic behaviors varied among the tested compounds, although the nonspecific mechanism of action against lipid membranes in general should be taken into account when considering application possibilities.

It should be emphasized that the QCM-D experiments were performed under continuous flow conditions, so the effects of compound concentration primarily relate to the aggregation state of the compound rather than the total amount of compound in the system. The addition of compounds at bulk concentrations below the corresponding CMC value appears to be insufficient to induce significant changes in membrane morphology even at longer time scales. This observation is consistent with a previous report by Thid et al.,[40] which supports that the micellar form is important for membrane disruption by the tested compounds. It was speculated that the micellar form provides surfactant aggregates which are needed to facilitate membrane remodeling or to serve as a reservoir source of monomers.[40] In other studies (see, e.g., ref 13), it has been shown that fatty acids encapsulated in liposomes destabilize bacterial cell membranes. Taken together, existing studies support that surfactant aggregation is important for membrane destabilization, and suitable formulations have been devised either spontaneously (micelles forming above the CMC, as in the present study) or through encapsulation (embedded in liposome bilayers).

In this regard, the membrane charge selectivity of the tested compounds also merits attention in the context of understanding the biological relevance of the experimentally observed membrane morphological responses. In the present study, the supported lipid bilayer was composed of single-component zwitterionic DOPC lipids in order to present a simplified and well-controlled model system. The results prove insightful in distinguishing various types of morphological changes in response to the surfactants. Looking forward, it is important to further understand how the tested compounds and other antimicrobial surfactants act against bacterial and human cell membranes. Both bacterial and human cell membranes exhibit complex structures and are composed of multiple types of zwitterionic and anionic lipids along with sterols (ref 23 and references therein). In general, bacterial cell membranes are regarded as possessing greater anionic character while the outer leaflet of the human cell plasma membranes is primarily zwitterionic. In some cases, cationic antimicrobials exhibit selective targeting of bacterial cell membranes on the basis of membrane surface charge. Taking into account that the tested compounds are either zwitterionic or anionic, membrane charge selectivity is not expected. Nevertheless, the interaction of fatty acids and related compounds using supported lipid bilayers with more complex membrane compositions, including the presence of sterols which influence membrane rigidity, could provide deeper insight into the extent of membrane morphological changes in biologically relevant lipid membranes. Furthermore, it is important to explore delivery vehicles

DOI: 10.1021/acs.langmuir.5b02088
Langmuir 2015, 31, 10223−10232

such as liposomes (cf. Introduction) and solid lipid nanoparticles[44] in order to encapsulate fatty acids and reduce potential human cell toxicities for application purposes.

CONCLUSIONS

In this work, we investigated how a series of membrane-active surfactants—lauric acid, SDS, and GML—destabilize supported lipid bilayers. The combination of QCM-D and fluorescence microscopy experiments allowed us to identify that each compound induces membrane morphological changes through a distinctive process which involves the formation of spherical or tubular protrusions out of the lipid bilayer. The measurement results support that the tested compounds induce membrane morphological responses primarily above the respective CMC values. The measured MIC values of each compound against standard and methicillin-resistant *S. aureus* bacterial strains further suggest that the compounds inhibit bacterial growth via membrane lysis. Taken together, the experimental findings demonstrate that the tested membrane-active surfactants can induce a spectrum of membrane morphological changes in supported lipid bilayers. Future work aimed at extending the scope of tested compounds and the biological relevance of the supported lipid bilayer platform could further improve our understanding of how membrane-active surfactants act against bacterial cell membranes and other lipid membranes.

ASSOCIATED CONTENT

Supporting Information

The Supporting Information is available free of charge on the ACS Publications website at DOI: 10.1021/acs.langmuir.5b02088.

Descriptions of Videos S1−S6, showing the time-lapse recording of surfactant-induced changes in lipid bilayer morphology (PDF)
Video S1 (ZIP)
Video S2 (ZIP)
Video S3 (ZIP)
Video S4 (ZIP)
Video S5 (ZIP)
Video S6 (ZIP)

AUTHOR INFORMATION

Corresponding Author

*E-mail: njcho@ntu.edu.sg.

Notes

The authors declare no competing financial interest.

ACKNOWLEDGMENTS

This work was supported by a National Research Foundation Fellowship Grant (NRF-NRFF2011-01) and an A*STAR-NTU-NHG Skin Research Grant (SRG/14028). J.A.J. is a recipient of the Nanyang President's Graduate Scholarship.

REFERENCES

(1) Laxminarayan, R.; Duse, A.; Wattal, C.; Zaidi, A. K.; Wertheim, H. F.; Sumpradit, N.; Vlieghe, E.; Hara, G. L.; Gould, I. M.; Goossens, H. Antibiotic resistance—the need for global solutions. *Lancet Infectious Diseases* **2013**, *13* (12), 1057−1098.

(2) Alanis, A. J. Resistance to antibiotics: are we in the post-antibiotic era? *Arch. Med. Res.* **2005**, *36* (6), 697−705.

(3) Heerklotz, H. Interactions of surfactants with lipid membranes. *Q. Rev. Biophys.* **2008**, *41* (3−4), 205−264.

(4) Davies, J.; Davies, D. Origins and evolution of antibiotic resistance. *Microbiology and Molecular Biology Reviews* **2010**, *74* (3), 417−433.

(5) Desbois, A. P.; Smith, V. J. Antibacterial free fatty acids: activities, mechanisms of action and biotechnological potential. *Appl. Microbiol. Biotechnol.* **2010**, *85* (6), 1629−1642.

(6) Hammer, K. A.; Carson, C. F. Antibacterial and Antifungal Activities of Essential Oils. In *Lipids and Essential Oils as Antimicrobial Agents*; John Wiley & Sons, Ltd., 2011; pp 255−306.

(7) Strandberg, K. L.; Peterson, M. L.; Lin, Y.-C.; Pack, M. C.; Chase, D. J.; Schlievert, P. M. Glycerol monolaurate inhibits *Candida* and *Gardnerella vaginalis In vitro* and *In vivo* but not *Lactobacillus*. *Antimicrob. Agents Chemother.* **2010**, *54* (2), 597−601.

(8) Thormar, H.; Hilmarsson, H.; Bergsson, G. Stable concentrated emulsions of the 1-monoglyceride of capric acid (monocaprin) with microbicidal activities against the food-borne bacteria *Campylobacter jejuni*, *Salmonella spp.*, and *Escherichia coli*. *Appl. Environ. Microbiol.* **2006**, *72* (1), 522−526.

(9) Yang, D.; Pornpattananangkul, D.; Nakatsuji, T.; Chan, M.; Carson, D.; Huang, C.-M.; Zhang, L. The antimicrobial activity of liposomal lauric acids against *Propionibacterium acnes*. *Biomaterials* **2009**, *30* (30), 6035−6040.

(10) Huang, C.-M.; Chen, C.-H.; Pornpattananangkul, D.; Zhang, L.; Chan, M.; Hsieh, M.-F.; Zhang, L. Eradication of drug resistant *Staphylococcus aureus* by liposomal oleic acids. *Biomaterials* **2011**, *32* (1), 214−221.

(11) Obonyo, M.; Zhang, L.; Thamphiwatana, S.; Pornpattananangkul, D.; Fu, V.; Zhang, L. Antibacterial activities of liposomal linolenic acids against antibiotic-resistant *Helicobacter pylori*. *Mol. Pharmaceutics* **2012**, *9* (9), 2677−2685.

(12) Pornpattananangkul, D.; Fu, V.; Thamphiwatana, S.; Zhang, L.; Chen, M.; Vecchio, J.; Gao, W.; Huang, C. M.; Zhang, L. *In vivo* treatment of *Propionibacterium acnes* infection with liposomal lauric acids. *Adv. Healthcare Mater.* **2013**, *2* (10), 1322−1328.

(13) Jung, S. W.; Thamphiwatana, S.; Zhang, L.; Obonyo, M. Mechanism of Antibacterial Activity of Liposomal Linolenic Acid against *Helicobacter pylori*. *PloS One* **2015**, *10* (3), e0116519.

(14) Thamphiwatana, S.; Gao, W.; Obonyo, M.; Zhang, L. *In vivo* treatment of *Helicobacter pylori* infection with liposomal linolenic acid reduces colonization and ameliorates inflammation. *Proc. Natl. Acad. Sci. U. S. A.* **2014**, *111* (49), 17600−17605.

(15) Kabara, J.; Vrable, R.; Jie, M. L. K. Antimicrobial lipids: natural and synthetic fatty acids and monoglycerides. *Lipids* **1977**, *12* (9), 753−759.

(16) Kabara, J. J. Structure-function relationships of surfactants as antimicrobial agents. *Journal of the Society of Cosmetic Chemists* **1978**, *29*, 733−741.

(17) Kabara, J. J. Antimicrobial agents derived from fatty acids. *J. Am. Oil Chem. Soc.* **1984**, *61* (2), 397−403.

(18) Kabara, J. J.; Swieczkowski, D. M.; Conley, A. J.; Truant, J. P. Fatty acids and derivatives as antimicrobial agents. *Antimicrob. Agents Chemother.* **1972**, *2* (1), 23−28.

(19) Conley, A. J.; Kabara, J. J. Antimicrobial action of esters of polyhydric alcohols. *Antimicrob. Agents Chemother.* **1973**, *4* (5), 501−506.

(20) Kabara, J. J. GRAS antimicrobial agents for cosmetic products. *Journal of the Society of Cosmetic Chemists* **1980**, *31*, 1−10.

(21) Howett, M.; Neely, E.; Christensen, N.; Wigdahl, B.; Krebs, F.; Malamud, D.; Patrick, S.; Pickel, M.; Welsh, P.; Reed, C. A broad-spectrum microbicide with virucidal activity against sexually transmitted viruses. *Antimicrob. Agents Chemother.* **1999**, *43* (2), 314−321.

(22) Nazari, M.; Kurdi, M.; Heerklotz, H. Classifying surfactants with respect to their effect on lipid membrane order. *Biophys. J.* **2012**, *102* (3), 498−506.

(23) Herzog, I. M.; Fridman, M. Design and synthesis of membrane-targeting antibiotics: from peptides-to aminosugar-based antimicrobial cationic amphiphiles. *MedChemComm* **2014**, *5* (8), 1014−1026.

DOI: 10.1021/acs.langmuir.5b02088
Langmuir 2015, 31, 10223−10232

(24) Bergsson, G.; Arnfinnsson, J.; Steingrímsson, Ó.; Thormar, H. Killing of Gram-positive cocci by fatty acids and monoglycerides. *APMIS* **2001**, *109* (10), 670−678.
(25) Mukerjee, P.; Mysels, K. J. A Re-evaluation of the Spectral Change Method of Determining Critical Micelle Concentration. *J. Am. Chem. Soc.* **1955**, *77* (11), 2937−2943.
(26) Inácio, Â. S.; Mesquita, K. A.; Baptista, M.; Ramalho-Santos, J.; Vaz, W. L.; Vieira, O. V. *In vitro* surfactant structure-toxicity relationships: implications for surfactant use in sexually transmitted infection prophylaxis and contraception. *PLoS One* **2011**, *6* (5), e19850.
(27) Jackman, J. A.; Cho, N.-J.; Duran, R. S.; Frank, C. W. Interfacial binding dynamics of bee venom phospholipase A_2 investigated by dynamic light scattering and quartz crystal microbalance. *Langmuir* **2010**, *26* (6), 4103−4112.
(28) Mechler, A.; Praporski, S.; Atmuri, K.; Boland, M.; Separovic, F.; Martin, L. L. Specific and selective peptide-membrane interactions revealed using quartz crystal microbalance. *Biophys. J.* **2007**, *93* (11), 3907−3916.
(29) Mashaghi, A.; Mashaghi, S.; Reviakine, I.; Heeren, R. M.; Sandoghdar, V.; Bonn, M. Label-free characterization of biomembranes: from structure to dynamics. *Chem. Soc. Rev.* **2014**, *43* (3), 887−900.
(30) Chambers, H. F.; DeLeo, F. R. Waves of resistance: *Staphylococcus aureus* in the antibiotic era. *Nat. Rev. Microbiol.* **2009**, *7* (9), 629−641.
(31) Rodahl, M.; Höök, F.; Krozer, A.; Brzezinski, P.; Kasemo, B. Quartz crystal microbalance setup for frequency and Q-factor measurements in gaseous and liquid environments. *Rev. Sci. Instrum.* **1995**, *66* (7), 3924−3930.
(32) Tabaei, S. R.; Choi, J.-H.; Haw Zan, G.; Zhdanov, V. P.; Cho, N.-J. Solvent-Assisted Lipid Bilayer Formation on Silicon Dioxide and Gold. *Langmuir* **2014**, *30* (34), 10363−10373.
(33) Jackman, J. A.; Zhao, Z.; Zhdanov, V. P.; Frank, C. W.; Cho, N.-J. Vesicle adhesion and rupture on silicon oxide: Influence of freeze−thaw pretreatment. *Langmuir* **2014**, *30* (8), 2152−2160.
(34) Zoraghi, R.; See, R. H.; Axerio-Cilies, P.; Kumar, N. S.; Gong, H.; Moreau, A.; Hsing, M.; Kaur, S.; Swayze, R. D.; Worrall, L. Identification of pyruvate kinase in methicillin-resistant *Staphylococcus aureus* as a novel antimicrobial drug target. *Antimicrob. Agents Chemother.* **2011**, *55* (5), 2042−2053.
(35) Wiegand, I.; Hilpert, K.; Hancock, R. E. Agar and broth dilution methods to determine the minimal inhibitory concentration (MIC) of antimicrobial substances. *Nat. Protoc.* **2008**, *3* (2), 163−175.
(36) Keller, C.; Kasemo, B. Surface specific kinetics of lipid vesicle adsorption measured with a quartz crystal microbalance. *Biophys. J.* **1998**, *75* (3), 1397−1402.
(37) Glasmästar, K.; Larsson, C.; Höök, F.; Kasemo, B. Protein adsorption on supported phospholipid bilayers. *J. Colloid Interface Sci.* **2002**, *246* (1), 40−47.
(38) Kelsey, J.; Bayles, K.; Shafii, B.; McGuire, M. Fatty acids and monoacylglycerols inhibit growth of *Staphylococcus aureus*. *Lipids* **2006**, *41* (10), 951−961.
(39) Tabaei, S. R.; Jackman, J. A.; Kim, S.-O.; Zhdanov, V. P.; Cho, N.-J. Solvent-Assisted Lipid Self-Assembly at Hydrophilic Surfaces: Factors Influencing the Formation of Supported Membranes. *Langmuir* **2015**, *31* (10), 3125−3134.
(40) Thid, D.; Benkoski, J. J.; Svedhem, S.; Kasemo, B.; Gold, J. DHA-induced changes of supported lipid membrane morphology. *Langmuir* **2007**, *23* (11), 5878−5881.
(41) Keller, S.; Heerklotz, H.; Blume, A. Monitoring lipid membrane translocation of sodium dodecyl sulfate by isothermal titration calorimetry. *J. Am. Chem. Soc.* **2006**, *128* (4), 1279−1286.
(42) Staykova, M.; Arroyo, M.; Rahimi, M.; Stone, H. A. Confined bilayers passively regulate shape and stress. *Phys. Rev. Lett.* **2013**, *110* (2), 028101.
(43) Israelachvili, J. N.; Mitchell, D. J.; Ninham, B. W. Theory of self-assembly of hydrocarbon amphiphiles into micelles and bilayers. *J. Chem. Soc., Faraday Trans. 2* **1976**, *72*, 1525−1568.
(44) Taylor, E. N.; Kummer, K. M.; Dyondi, D.; Webster, T. J.; Banerjee, R. Multi-scale strategy to eradicate *Pseudomonas aeruginosa* on surfaces using solid lipid nanoparticles loaded with free fatty acids. *Nanoscale* **2014**, *6* (2), 825−832.

DOI: 10.1021/acs.langmuir.5b02088
Langmuir 2015, 31, 10223−10232